273

31 pg — $1.00

TASK R
Quarterly Progress Report No. 21
for the period
1 April-30 June 1964

DDC

JUL 1 3 1964

DDC-IRA A

DISCLAIMER NOTICE

THIS DOCUMENT IS THE BEST
QUALITY AVAILABLE.

COPY FURNISHED CONTAINED
A SIGNIFICANT NUMBER OF
PAGES WHICH DO NOT
REPRODUCE LEGIBLY.

TASK R

Quarterly Progress Report No. 21
for the period
1 April-30 June 1964

Summary

Results from a large number of runs to measure
the $O-O_2$ diffusion coefficient in a flow tube are
discussed. The general behavior are non linear plots
of $\log (O)/(O)_o$ vs distance, indicating an overall
loss of O-atoms which is not first order. Possible
causes are discussed. A successful comparison of
relative O atom concentrations determined by ESR
signal peak heights and by monitoring the O-NO glow
with a photomultiplier is given.

Experiments with aerodynamic beams of He-Ar
mixtures in the prototype apparatus are described.
A final design for the crossed beam apparatus is
given and the various specifications of the beams
are estimated. Some simple design criteria for
aerodynamic beams are outlined.

Recent experience with the high temperature CO_2
calibration equipment for the fast scanning infrared
spectrometer is described. Both a heated free jet
and a static cell have been used. Reproducibility of
the technique was demonstrated by a repeat of an
earlier rocket tunnel test run, the CO_2 absorption
at 4.24μ at the 1.35" station checking with 0.1%.

GENERAL OBJECTIVES OF TASK R

It seems likely that long-range development of improved propulsion systems will rely more and more upon a sound understanding and quantitative knowledge of the underlying physical and chemical phenomena involved. Many of these phenomena, and the practical problems arising in connection with them, have to do with the high temperatures characteristic of most advanced propulsion systems. Prediction of performance, the problems encountered with materials, heat transfer and cooling techniques - all these become more difficult and sophisticated with the trend to higher temperature operation, and will ultimately require a more fundamentally based understanding than is characteristic of the usual expensive "cut-and-try" or "quick-fix" test procedures.

Research performed under Task R at the Applied Physics Laboratory is intended to provide some of this basic knowledge in appropriate areas. The general emphasis is on the physico-chemical and fluid dynamic behavior of high temperature, high speed gas flows such as occur in most advanced propulsion systems.

A. A. Westenberg
Program Coordinator

I. DISSOCIATED GAS STUDIES

(N. de Haas and A. A. Westenberg)

Objective

Several aspects of the high temperature gas flow associated with most propulsion systems have to do with the behavior of dissociated gases containing various labile atoms and radicals. Heat transfer and mixing processes often involve the diffusion of such species and their reactions in gas boundary layers and at surfaces. Because of their high reactivity, reliable basic data on the transport and kinetic properties of atoms and radicals are difficult to obtain. The difficulties lie both in establishing a well-defined experimental system appropriate to the measurement to be carried out and in detecting and measuring the labile species themselves.

The objective of the present program is to utilize the flow tube technique to study the diffusion and chemical kinetics of discharge-generated atoms and radicals under well-defined conditions. The detection system to be employed is that of electron spin resonance (ESR), since the unpaired electron(s) possessed by all free radicals makes this technique the most widely applicable of any presently available. Previous work has demonstrated that ESR can be used as a quantitative detector of atoms and radicals in the gas phase.

Experimental

In the previous Quarterly Report (Ref. 1) the theory for measuring labile atom-molecule diffusion coefficients in a flow tube was outlined in detail and an experimental apparatus described which utilized ESR s the detector for the labile atoms. During the present period a great number of experiments were performed with the system which will be discussed more or less in chronological order.

A number of runs on the $O-O_2$ system to determine the O-atom concentration gradient along the tube with flow and under static conditions practically always showed non linear logarithmic plots, i.e. log (O) vs distance (z). The theory predicated upon first order atom loss and constant source strength requires that such log plots should be linear, whereas the experimental result was that the slope tended to increase with distance away from the atom source (the discharge cavity), although it usually became linear after a distance of 20-30 cm. Thinking that this behavior was probably due to electronically excited O_2 generating O atoms outside the discharge, as recent evidence suggests (Ref. 2), the apparatus was altered slightly as shown in Fig. I-1. Instead of putting the discharge source of atoms directly on the flow tube as in Fig. I-1 of Ref. (1), it was installed on a sidearm off from the main flow tube as shown here. It was hoped that this longer effective path length from the discharge would give more chance for the excited O_2 to decay before the atom gradients were measured.

The sidearm was originally situated perpendicular to the flow tube as shown in Fig. I-1 by the dashed lines. When log plots of (O) vs z were still strongly nonlinear as before it was then suspected that the extraneous field from the 9-inch magnet of the ESR spectrometer might be influencing the discharge. This proved to be the case (later verified by monitoring the O-NO glow with a photomultiplier held at a fixed position downstream as the magnet was moved) since when the sidearm was bent back as shown farther out of the residual field, the log plots usually became
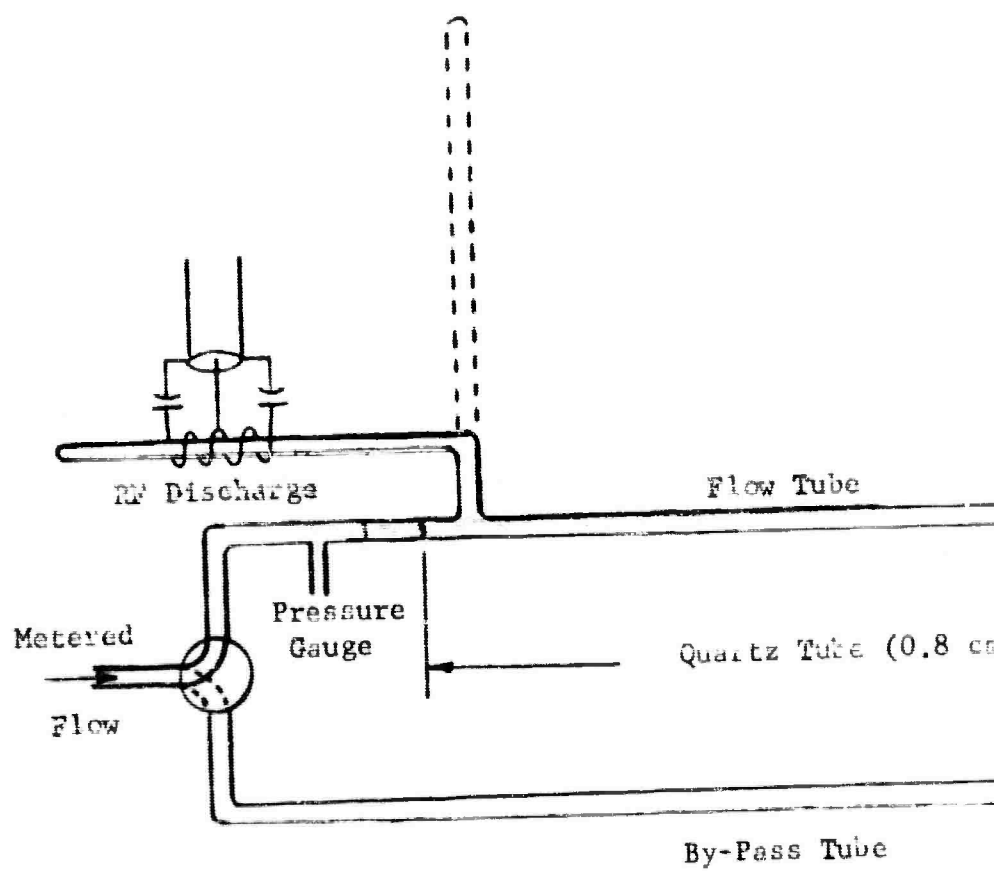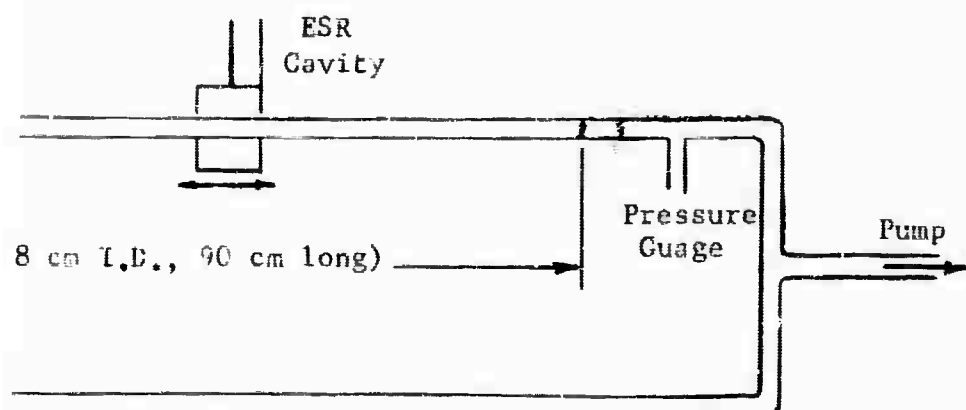
RF Discharge

Flow Tube

Pressure
Gauge

Metered

Flow

Quartz Tube (0.8 cm

By-Pass Tube

Fig. I-1. Schematic of Atom Di

ESR
Cavity
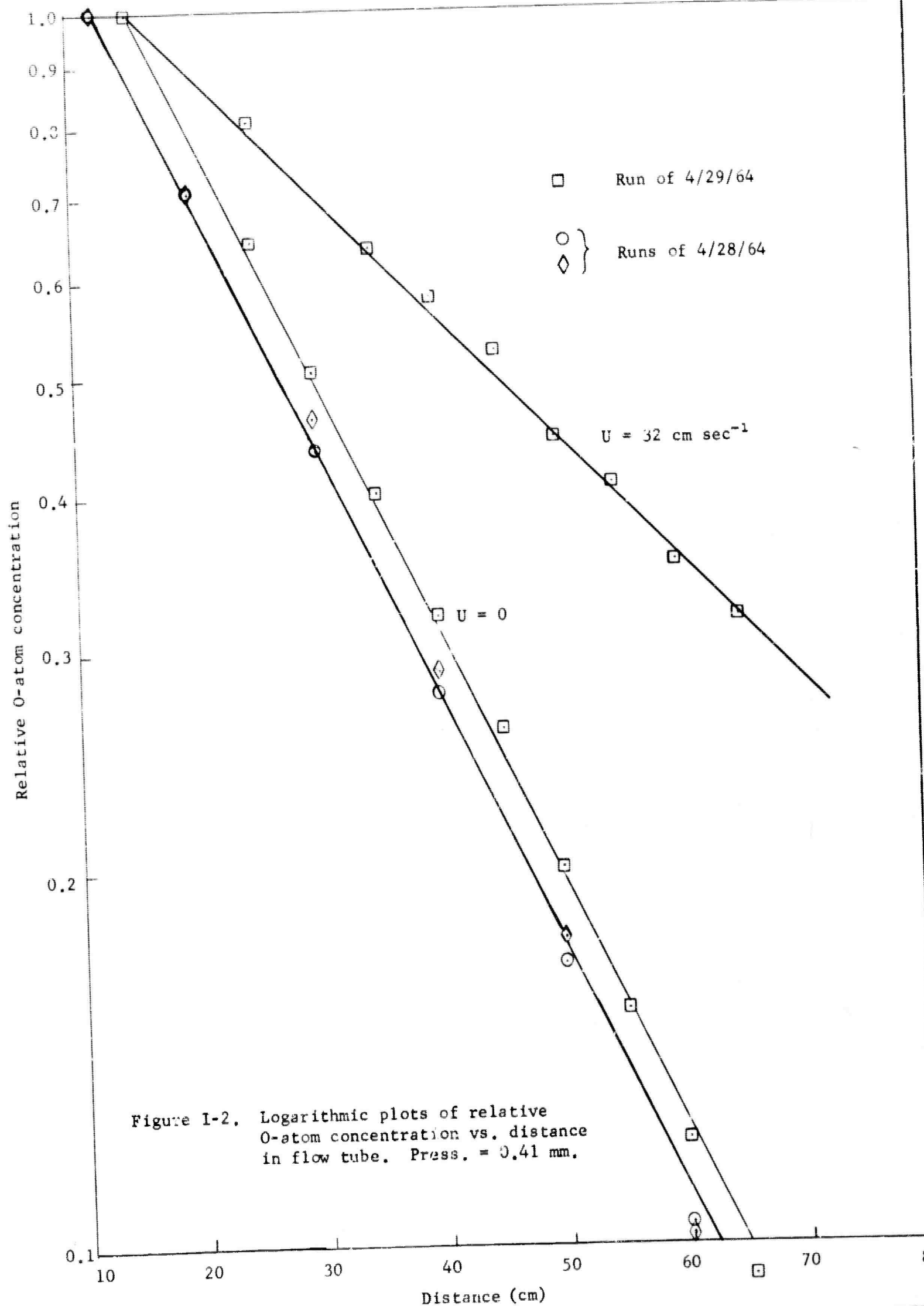
Pressure
Guage

Pump

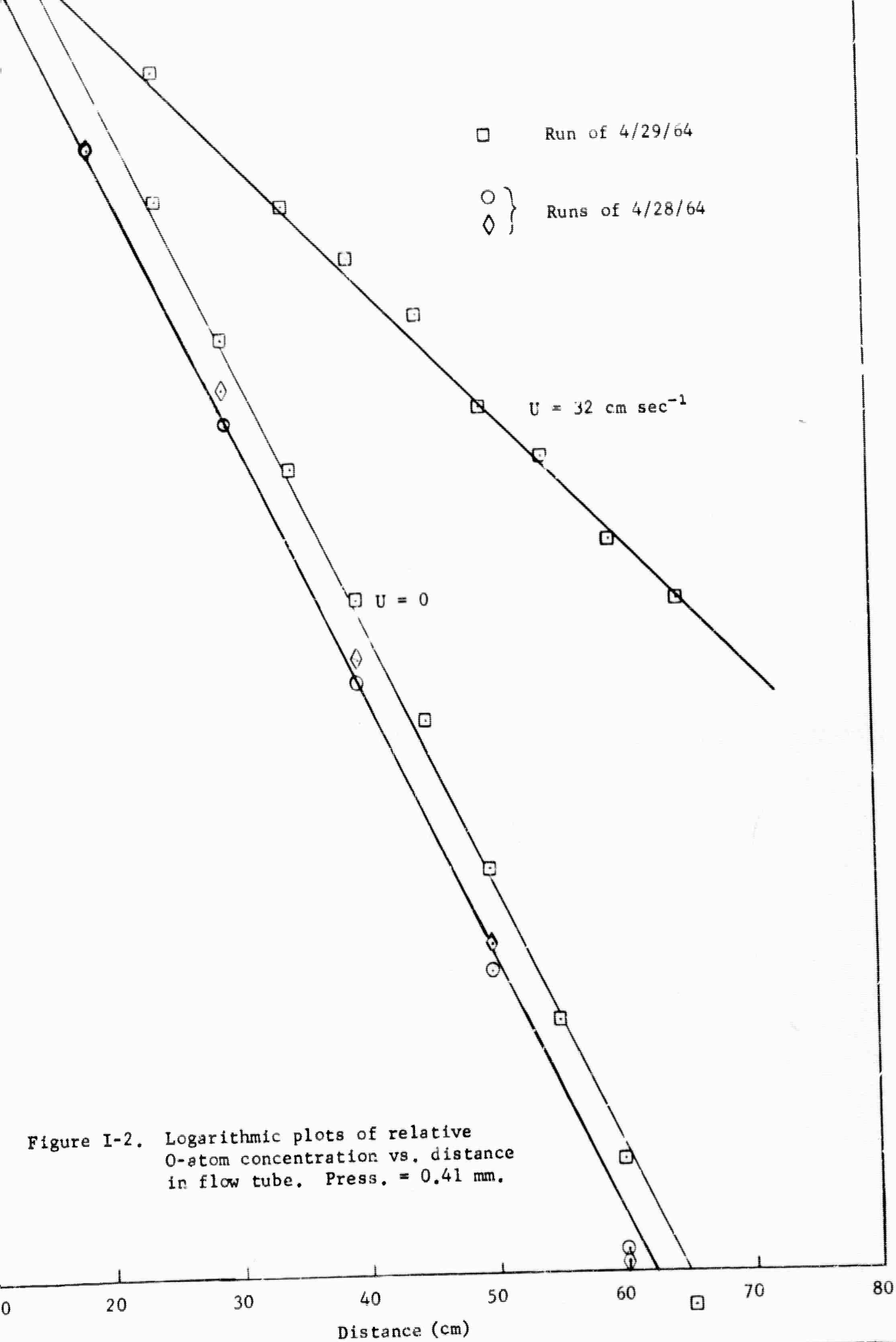8 cm I.D., 90 cm long)

Diffusion Apparatus.

essentially linear. Apparently the effect of the field (which must have been very small) when the magnet was close enough to the discharge was to reduce the atom source strength - probably by causing electrons in the discharge to move to the wall and be lost. It was also decided that a 28 mc. RF discharge source was more stable at lower pressures than the 2450 mc. microwave source which had been used previously.

The usual procedure with the apparatus was then to leave the O_2 flowing in the bypass or flow-through conditions with the discharge on overnight, so as to attain a thoroughly steady "cleaned out" state in the system. The next day the atom gradient would be measured and the flow switched to the other condition (flow or bypass) and the gradient measured after enough time for the system to steady down (usually only about an hour). An example of the gradients obtained in this way, and their reproducibility, is shown in Fig. I-2. The three static runs were taken on two consecutive days and show excellent reproducibility.

A number of runs at different pressures and flow rates did not, however, give the same apparent $O-O_2$ diffusion coefficient when computed by the theory outlined in Ref. (1). The values of D_{O-O_2} obtained ranged over 0.15-0.4 cm^2 sec^{-1} (corrected to P = 1 atm) which is clearly unacceptable. Furthermore, the static slopes themselves did not seem to plot smoothly against pressure as they should have if they represented decays governed by the expected homogeneous and heterogeneous kinetic mechanisms.

In casting about for explanations of the difficulty, it was decided to make one additional check that the ESR method using the peak-to-peak signals was indeed measuring correct relative atom concentrations. Provision was made for discharging the O_2 far upstream of the sidearm (not used for this experiment) and injecting a trace of NO at the entrance to the flow tube (so the NO did not enter the discharge - an important point). The O atom gradients could then be measured independently by means of a photomultiplier mounted so that it could be traversed along the flow tube at the same time that the ESR detector cavity and magnet were moved. Comparisons of the ESR and NO-photomultiplier measured O atom

Figure I-2. Logarithmic plots of relative
O-atom concentration vs. distance
in flow tube. Press. = 0.41 mm.

Run of 4/29/64

$\left.\begin{array}{c} \circ \\ \Diamond \end{array}\right\}$ Runs of 4/28/64

$U = 32$ cm sec^{-1}

$U = 0$

Figure I-2. Logarithmic plots of relative
O-atom concentration vs. distance
in flow tube. Press. = 0.41 mm.

Distance (cm)

concentration gradients (normalized to the same point in the flow tube) at two different pressures and flow rates are shown in Fig. I-3. The agreement is excellent and leaves no doubt that the ESR and photomultiplier are both independently measuring the same relative O atom concentrations correctly.

The reason for the inconsistency of the measured values of D_{O-O_2} remains unexplained. It may be that the effect of excited O_2 is actually significant in generating O down the length of the tube, but does not show up much in the log plots over one or one and a half powers of ten in atom concentration. A close examination of Fig. I-2 shows that the measured (O) values seem to drop off slightly at the right hand end of the plot, which may be an indication that the loss rate is not strictly first-order in (O). This, of course, would make the theory inapplicable and could cause inconsistencies in the apparent first-order slopes, and hence the diffusion coefficients. Some additional experiments were run with a few percent of O_2 dissociated in a main flow of argon, where presumably any difficulty with excited O_2 would be avoided. These experiments also gave inconsistent results for D_{O-Ar}, however, which would tend to cast doubt on the excited O_2 explanation. A few runs in $H-H_2$ mixtures gave strongly curved log plots from which no firm conclusions could be drawn, since it was not certain that the magnetic field was not affecting the discharge in these runs. The diffusion experiments are being suspended for a while pending an explanation of the basic inconsistency of the measurements.

References

1. Task R Quarterly Progress Report No. 20 for the period 1 Jan. - 31 March 1964. APL/JHU Report SR 4-4.

2. F. Kaufman and J. R. Kelso, J. Chem. Phys. 40, 1152 (1964).
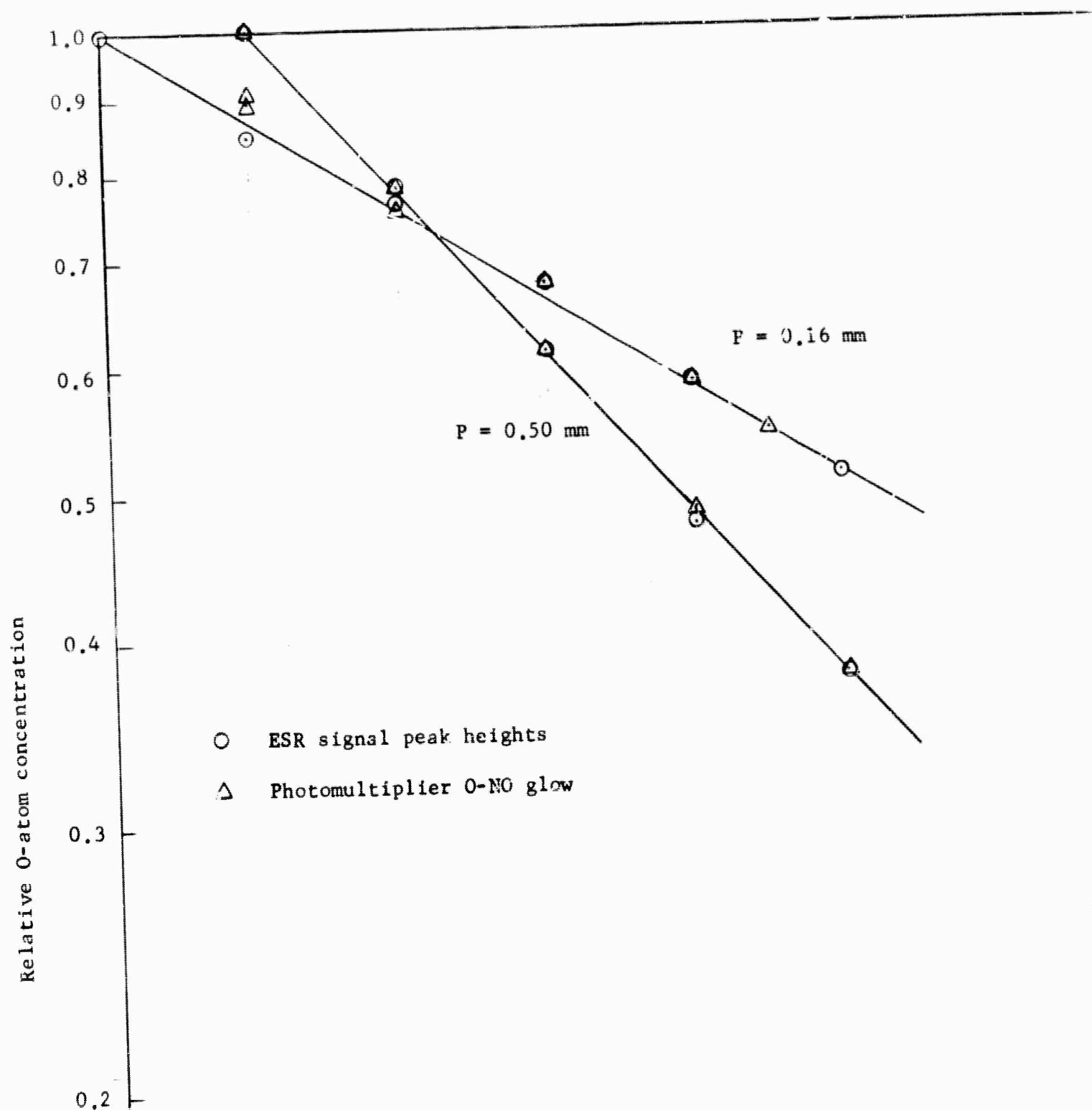
Figure I-3. Comparison of logarithmic O-atom gradients in flow tube determined by ESR (signal peak height) and by photomultiplier measurement of O-NO glow.

II. MOLECULAR BEAM CHEMICAL KINETIC STUDIES

(R. M. Fristrom and C. Grunfelder)

Objective

Reactions between molecules in the form of beams of well-defined energies offer an attractive way to study chemical kinetics of elementary reactions. By analysis of the scattered product distribution from two such interacting beams, it is possible to derive data on the activation energy and steric factor of the reaction. In this project, it is intended to develop the technique of generating and using aerodynamic beams for such purposes.

Recent Progress

During the past quarter progress was made on a number of facets of the program. Final designs for the crossed beam apparatus were completed and assembly is scheduled for the coming quarter. Realizable beam intensity and velocity in the prototype apparatus were raised by use of helium as a light gas driver. A discharge tube was constructed and is under test as a molecular beam source of atoms. The time delay circuit for velocity measurement was incorporated into the spectrometer. A solid state photovoltaic cell with improved frequency response was tested for the beam synchronizing pulse and found satisfactory. Velocity distribution test runs will be undertaken using the modified equipment. Some simple design criteria were developed for aerodynamically accelerated molecular beams.

Design of Crossed Beam Apparatus

As was indicated in the previous quarterly report, the attainable beam strengths appear to be great enough to perform scattering experiments using the mass spectrometer as a detector. Therefore, the time seemed ripe for freezing of the design, construction, and assembly of the crossed beam apparatus. Many of the parts have already been constructed and tests, e.g., the main vacuum chamber and its mounting table, the chopping wheel and motor, the rotatable mount, and, of course, the mass spectrometer detector. On the other hand, a number of items are yet to be built and the assembly of the system is a major job.

The aim was to produce an apparatus which would allow a detailed study of the angular and velocity distribution of the molecular scattering from crossed beams of known narrow velocity distribution. From these basic data collision cross sections and intermolecular potentials can be derived from which the transport coefficients and chemical kinetic information can be derived.

The characteristics of the projected system are summarized in Table I. Diagrams of the system are given in Fig. II-1 and II-2. The design parameters are extrapolations of our experience with the prototype apparatus. They are conservative assuming the system operates as planned, but are optimistic in assuming that the system will operate as planned. If, as is hoped, a reasonable fraction of this capability is realized, the instrument will provide an exceedingly useful tool for studying scattering problems, elastic, inelastic, and reactive. A few words of explanation are in order concerning the meaning of the items in Table I and how they were estimated.

(1) Beam Constituents. To obtain an aerodynamically accelerated beam it is necessary that the constituent be a gas with a vapor pressure esceeding 1 cm of Hg. This is not a stringent limitation since an oven can be used to raise the system temperature.
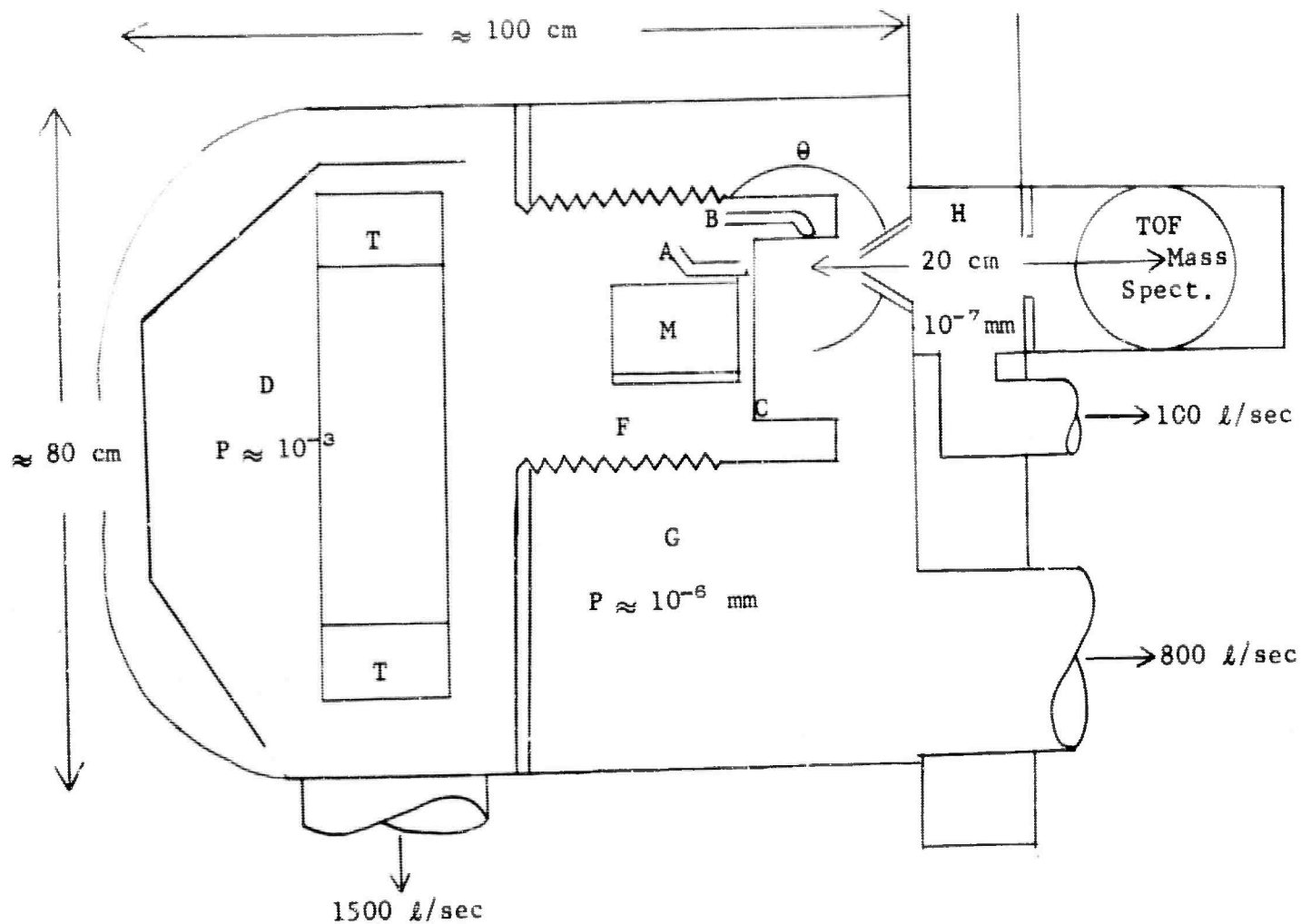
Fig. II-1. Schematic of Crossed Beam Apparatus.

A, B - Jet sources for crossed beams
C   - Chopping Wheel
D   - Jet Chamber
F   - Flexible Teflon Tube
G   - Crossed Beam Chamber
H   - Buffer Chamber
M   - 400 cps Chopping Motor
T   - Liquid N_2 Trap
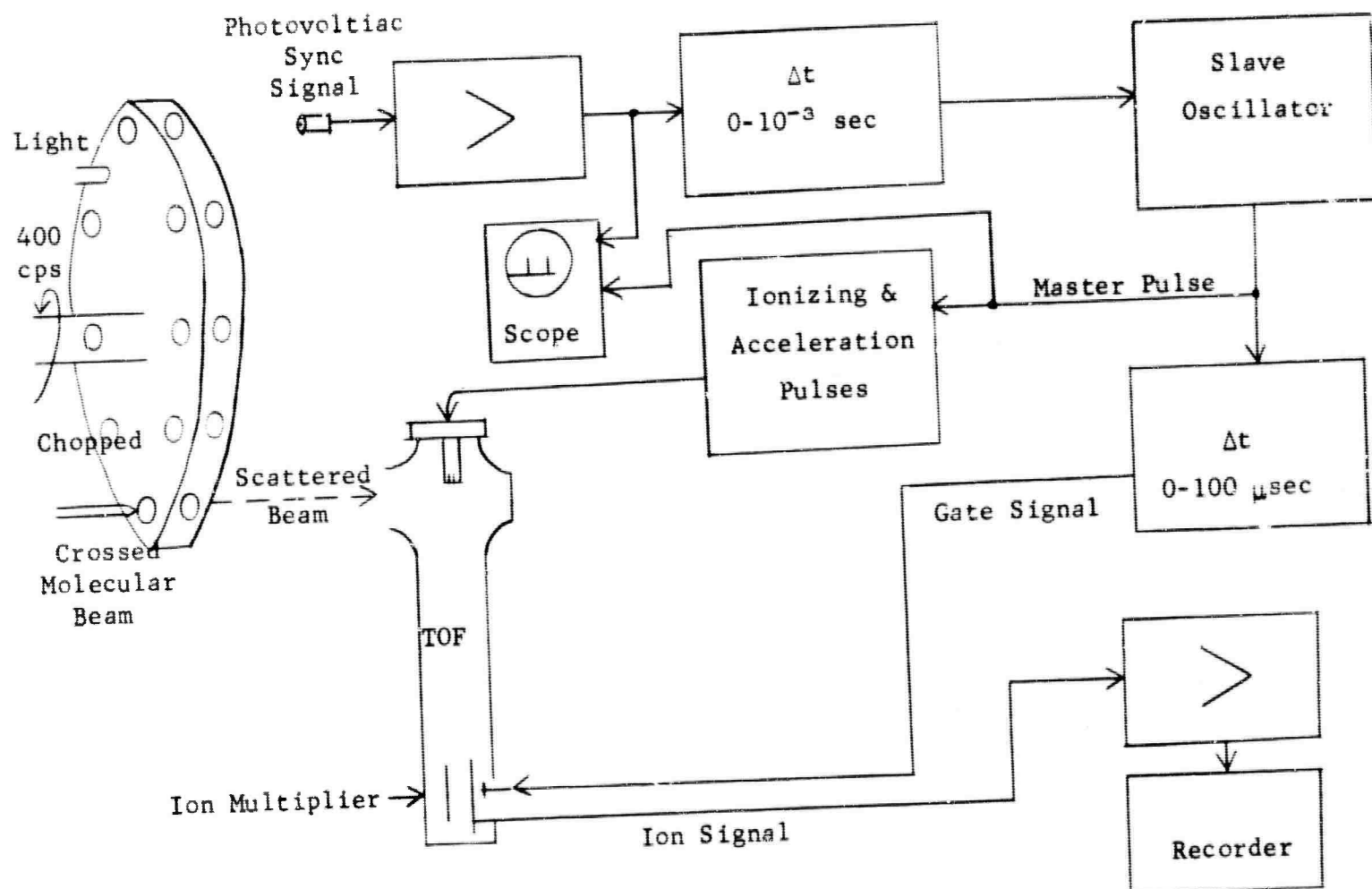θ   - Angle Positioned for Crossed Beam

Fig. II-2. Block Diagram of Crossed Molecular Beam Apparatus.

Table I. DESIGN CHARACTERISTICS OF CROSSED MOLECULAR BEAM APPARATUS.

(1) Beam Constituents.   Any molecular species whose vapor pressure
                                          can be raised above a few mm of Hg.

(2) Maximum Beam Density. 3×10^{19} molecules cm^{-2} sec^{-1}.

(3) Beam Cross Section.   0.5 cm X 0.2 cm.

(4) Beam Velocity. 10^4 to 2×10^5 cm/sec ($\pm$ 2%).

(5) Velocity Detection Range. 2×10^{16} cm/sec (3000 cycle mod.)
                                          10^3 cm/sec (50 cps mod.)

(6) Separation of Beam   Minimum 20 cm (maximum > 100 cm).
     Crossing and Detector.

(7) Beam Modulation Frequency.   50-3000 cps.

(8) Spectrometer Sensitivity. 10^{-12}mm of Hg (3×10^4 molecules/cm^3)
                                          (3×10^4v molecules/cm^2/sec flux)
                                          v is molecular velocity in cm/sec.

(9) Background Level. 10^{-10} mm of Hg.

(10) Scattering Probability of   0.1
     Beam.

(11) Dynamic Range of $> 10^6$:1.
     Detection.

(12) Angular Distribution of $\theta - 12^\circ - + 50^\circ$ ($\pm$ 3°), $\phi - + 12^\circ - - 12^\circ$
     Scattering. (See Fig. II-3)   ($\pm$ 1°)

---

(2) Maximum Beam Density. This is the density calculated for optimum conditions at the beam crossing point (see section on molecular beam design). Densities of this order have been realized by other groups and we have come within a factor of 5 in our preliminary experiments (see section on mixed beams).

(3) Beam Cross Section.

(4) Beam Velocity. Beam velocity is controlled by the temperature of the source ($v \approx 2.25$ v_o where v_o is the speed of sound in the gas). In the case of mixed beams the molecular weight is that of the mixture, so that an appreciable increase in sound velocity can be

obtained by driving a heavy gas with a light one such as helium. The critical velocity in chemical reactions is the relative velocity of the two beams. This depends on the angle of intersection which is initially set at 90°. This can be controlled so that the effective collisional velocity can be varied over an order of magnitude greater range than the indicated one. The velocity distribution in the beam is controlled by the transition flow Mach numbers. This usually exceeds Mach 10 and the halfwidth at half height is 3%.

(5) Velocity Detection Range. The instrument should be capable of detecting molecules with velocities in the laboratory coordinate system ranging from 10^3-10^6 cm/sec. The error dispersion stems from a distance ambiguity of 20 cm $\pm$ 0.5 cm and a time ambiguity of 5 microseconds or 2.5%. Thus the probable error will be 2.5% for velocities below 2×10^5 cm/sec; above this velocity the error will increase with velocity.

(6) Separation of Detector from Beam Crossing Point. This is fixed at the minimum value of 20 cm for initial experiments. It can be increased by installing a drift tube between the crossed beam apparatus and mass spectrometer. This would improve the precision of velocity measurements and allow detection of higher velocity molecules, but this is done at the expense of signal which varies inversely with the square of this distance.

(7) Beam Modulation Frequency. This variable can be controlled by changing the number of holes in the chopping wheel and the speed of the driving motor. Sensitivity of the instrument is proportional to the square root of this frequency. The chopping frequency determines the minimum molecular velocity which can be detected, so that a high modulation rate is appropriate for the study of high speed molecules and low modulation rate for low velocity molecules. Fortunately the sensitivity of the spectrometer and the pulse strength favor low modulation rates and more than compensate for the loss in sensitivity due to lower modulation rate. As a general rule, a particular velocity range should be studied at the maximum practical modulation rate.

(8) Spectrometer Sensitivity. In this experiment the measured quantity is local concentration while the desired quantity is flux or relative flux. To obtain flux from mass spectrometer measurements it is necessary to know the molecular velocity. The minimum detectable signal of our instrument is 10^{-12} mm of Hg (i.e. 3×10^4 molecules per cm^3). This density corresponds to a flux of $3 \times 10^4 v$ molecules per cm^2 per sec where v is the molecular velocity in cm per cm. It should be noted that the spectrometer sensitivity is inversely proportional to the molecular velocity.

(9) Background Level. Extrapolating experience in the present system to the larger pumping system of the crossed beam system it is estimated that the spectrometer background will be lower than 10^{-10} mm of Hg.

(10) Scattering Probability of the Beam. The estimate of a scattering probability of 0.1 is based on expected beam intensities and viscosity derived mean free paths. This is a measure of the strong scattering. Small angle scattering is several times more probable. Reactive scattering will, of course, be a small fraction of the total scattering.

(11) Dynamic Detection Range. This is the ratio of maximum to minimum detectable signal in terms of local density. Because the sensitivity of the instrument toward molecular flux varies with velocity (see above) the ratio of the strong unscattered beam (high velocity) to reaction products (often low velocity) may be as high as 10^8 to 1.

(12) Angular Distribution of Scattering. Much of the information obtainable from scattering experiments is contained in the angular distribution of species (the other important parameter is the velocity distribution). Therefore, the apparatus was designed to allow a maximum flexibility consistent with mechanical limitations in studying this distribution. To obtain the complete distribution it is not necessary to measure the whole sphere because the angle of scattering is more restricted in laboratory coordinates than it is in center of mass coordinates and, in general, conservation of momentum allows the inference of the distribution
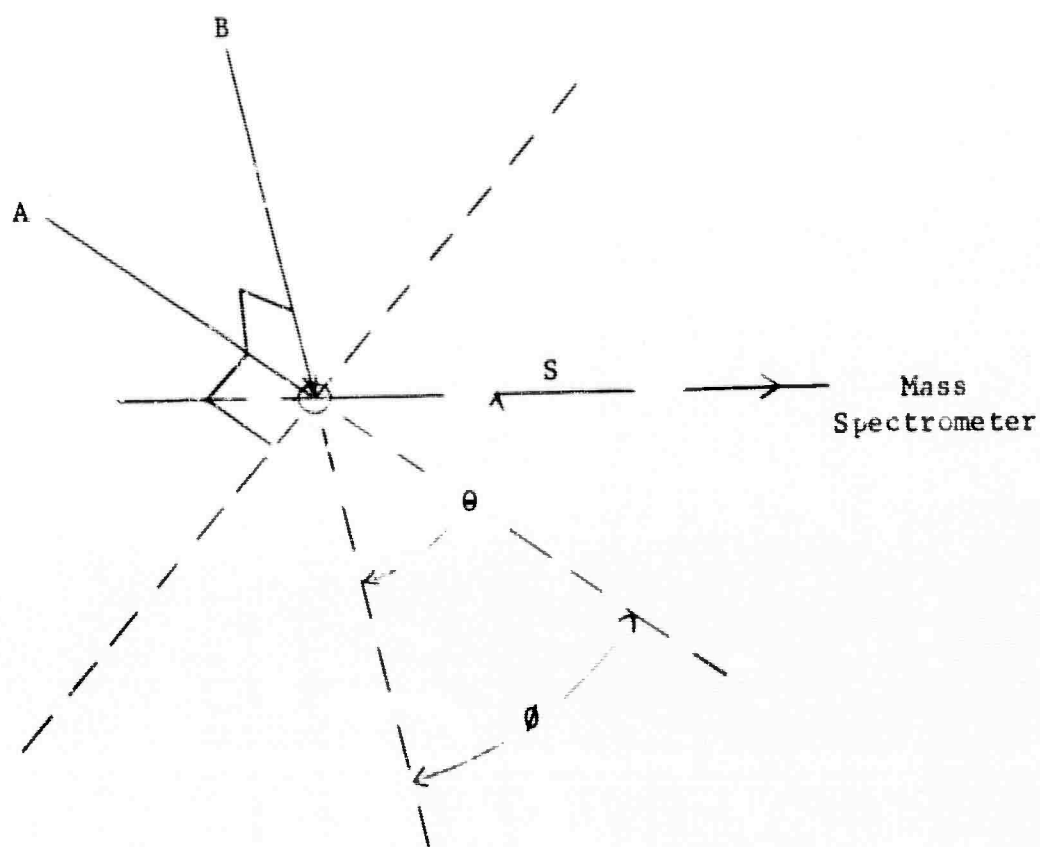
Fig. II-3. Geometry of Crossed Molecular Beam.

A - Molecular Beam A
B - Molecular Beam B
S - Scattering Beam to Mass Spectrometer
θ - Angle Between Scattering Beam to Mass
    Spectrometer and Plane Normal to Beam B
∅ - Angle Between Scattering Beam and
    Beam A in Normal Plane

of a component in an inaccessible angle from its complementary component distribution in an accessible region. By interchanging beams A and B and using conservation of momentum considerations it is believed that most of the pertinent information can be obtained.

Experiments on Prototype Apparatus

To furnish design information for the final apparatus a number of experiments have been run using the prototype apparatus described in previous reports. One very successful test was that of mixed beams. It has been observed by Becker, Fenn, and others (Refs. 1, 2) that if a beam of light gas with a trace of heavy component to be studied is used that the beam velocity is characteristic of the mixture (i.e. high velocity) and the separation occurs with a concentration of the heavy component along the axis. They observed that it was possible to obtain stronger beams of a heavy component using a trace in a light gas than was possible using the pure gas itself. A beam source of this type is desirable for several reaons. (1) Higher intensities appear possible. (2) Background interference is reduced because the predominant species will be the light carrier gas. (3) Higher collision energies are possible.

We have made several runs and found our experience parallels that previously reported. Stronger beams were possible using the mixed gas source (see Fig. II-4) and the background was considerably reduced. One interesting observation is that, in contrast with pure beams, the beam intensity realized increased monotonically with beam driving pressure unless the background pressure becomes comparable with the beam density at the skimmer. Realizable beam intensity shows a shallow maximum around 20 mole percent.

A discharge tube source for the production of molecular beams of atomic constituents was constructed and is undergoing tests.
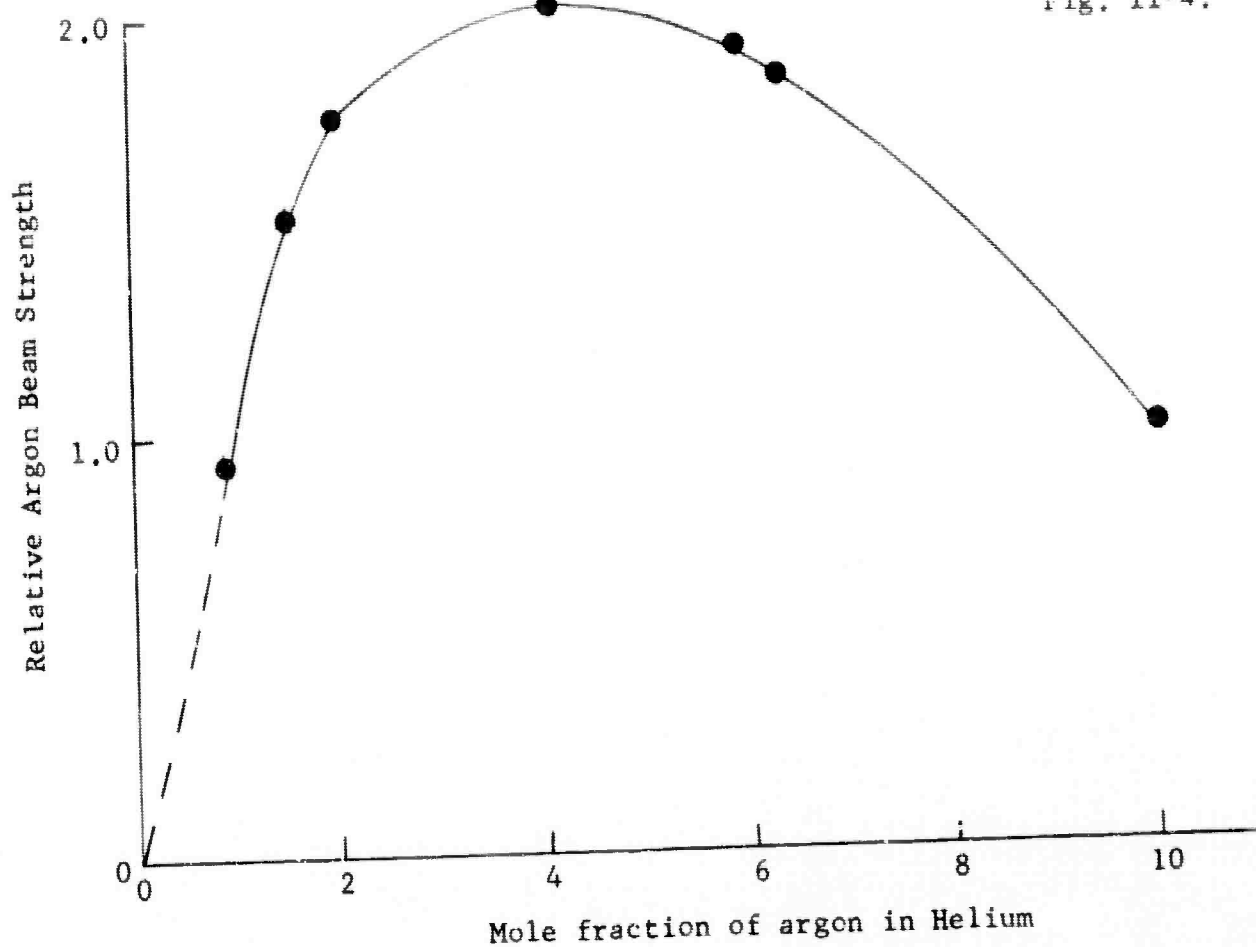
(a)

Fig. II-4.

Relative Argon Beam Strength

2.0

1.0

0

Mole fraction of argon in Helium

(b)

2.0

Relative Argon Beam Strength

$P_A < 10\mu$

$P_A = 400\mu$
(100 ℓ/sec)

$P_A \approx 100\text{-}500\mu$

1.0

$P_A < 20\mu$

— ● — 100 ℓ/sec diffusion pump

— X — 5 ℓ/sec mechanical pump
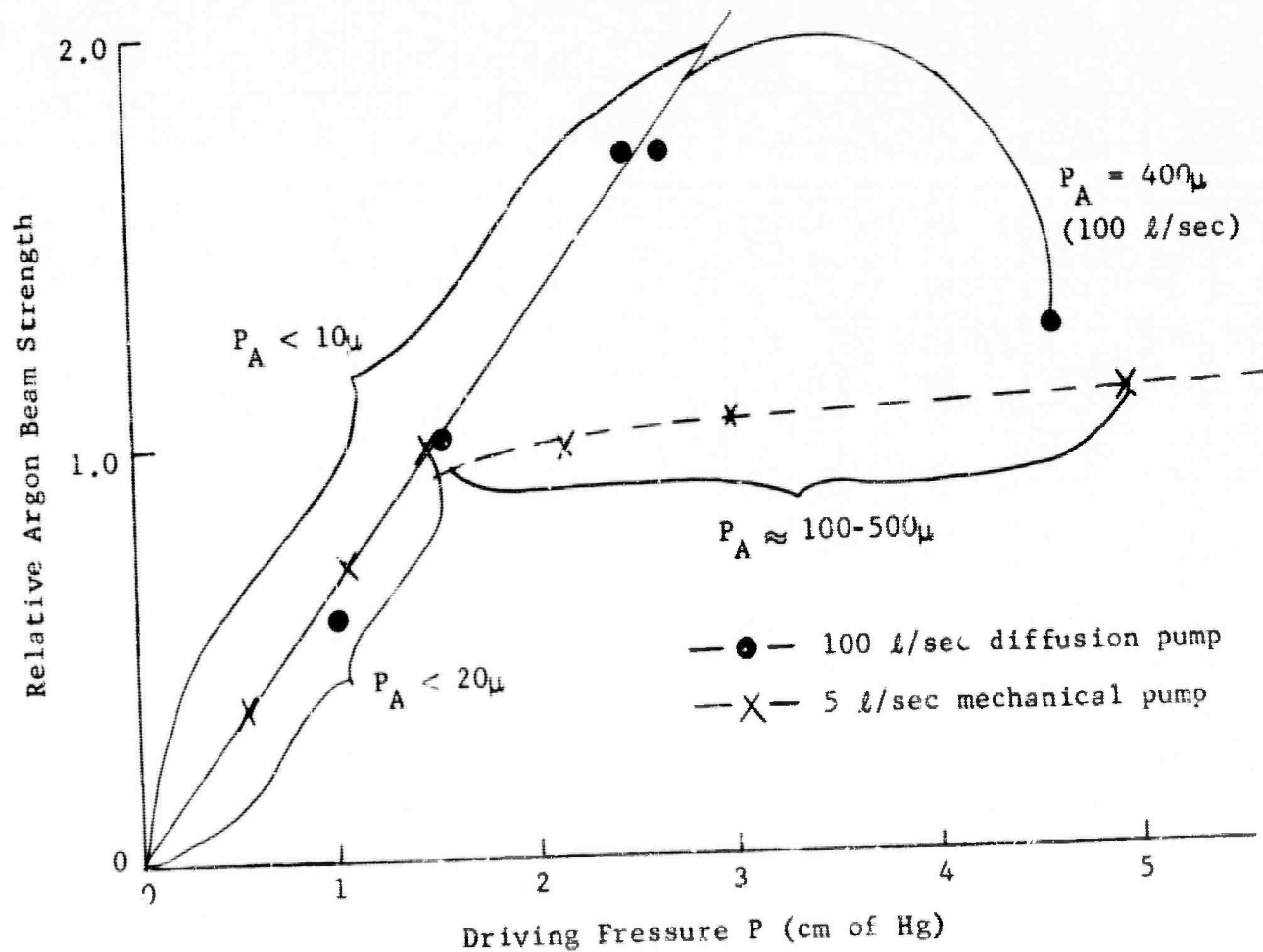
0

Driving Pressure P (cm of Hg)

Fig. II-4. a. Total Pressure Equals 2.87 cm.
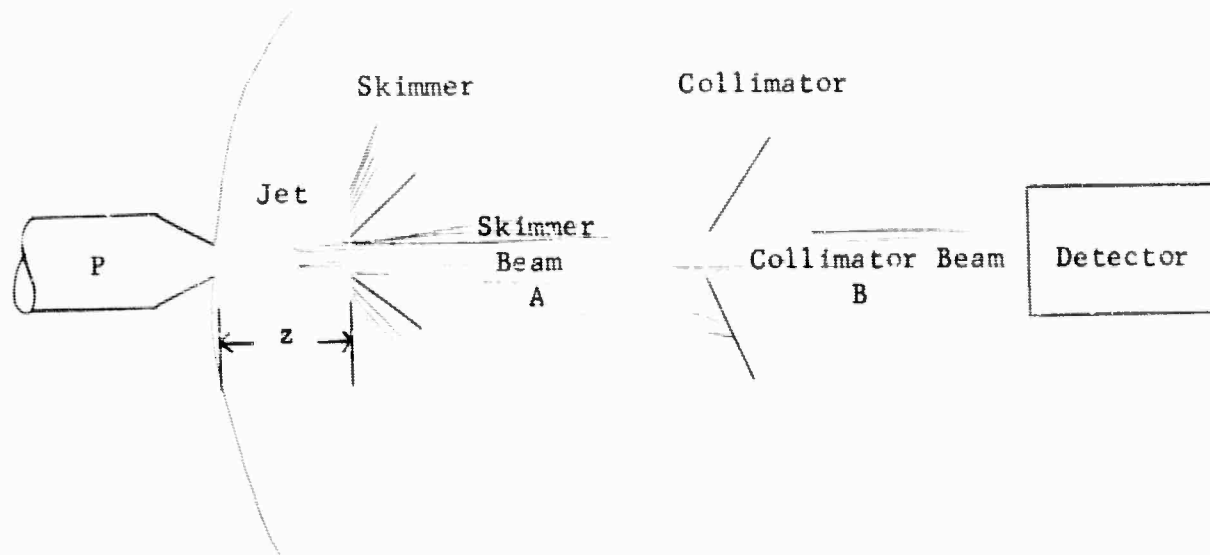   b. 80% He, 20% Ar. Comparison for Two Nozzle Chamber Pumps.

Apparatus

The time delay circuit which is to be used for the velocity measurements (Fig. II-2) was incorporated into the mass spectrometer. Delays ranging from a fraction of a microsecond to one millisecond are available. Longer delays than this can be accomodated mechanically in the new system. The present synchronization signal is derived from a photodiode of limited frequency response and the resulting jitter has prevented reliable velocity determinations. The spectrometer and delay circuit, however, behaved very well separately and the substitution of a photovoltaic synchronizer (Texas Instrument LS 223) which has 10 mega-cycle response should solve this problem.

Molecular Beam Design Principles

The behavior of aerodynamically accelerated molecular beam sources is rather imperfectly understood, so that the design of sources for these experiments is a rather empirical business. For this reason we have examined our own data and that published by others to see what regularities could be found to aid in our design.

Our molecular beam system is typical of that used by many investigators. It consists of a small convergent orifice, a conical skimmer and a detector. A secondary collimator exists between our skimmer and detector (this is also typical), but the flow in this region is pure molecular and well understood and will not affect the present discussion. The observed strength of the molecular beam depends on a number of factors: orifice area, skimmer area, separation between ori-fice and skimmer, driving pressure above the orifice, and the background pressures in the various pumping chambers (i.e. the pumping speed used). The observed beam intensity is a complex function of these variables (Ref. 5) (Fig. II-5). The size of the skimmer is usually dictated by the experiment, while the orifice size and driving pressure are limited by the available pumping speed.

a

Skimmer   Collimator

Jet

Skimmer
P   Beam   Collimator Beam   Detector
A   B

z

b

P_{opt}

Beam Strength

$P > P_{opt}$

$P < P_{opt}$

Nozzle - Skimmer Separation (z)
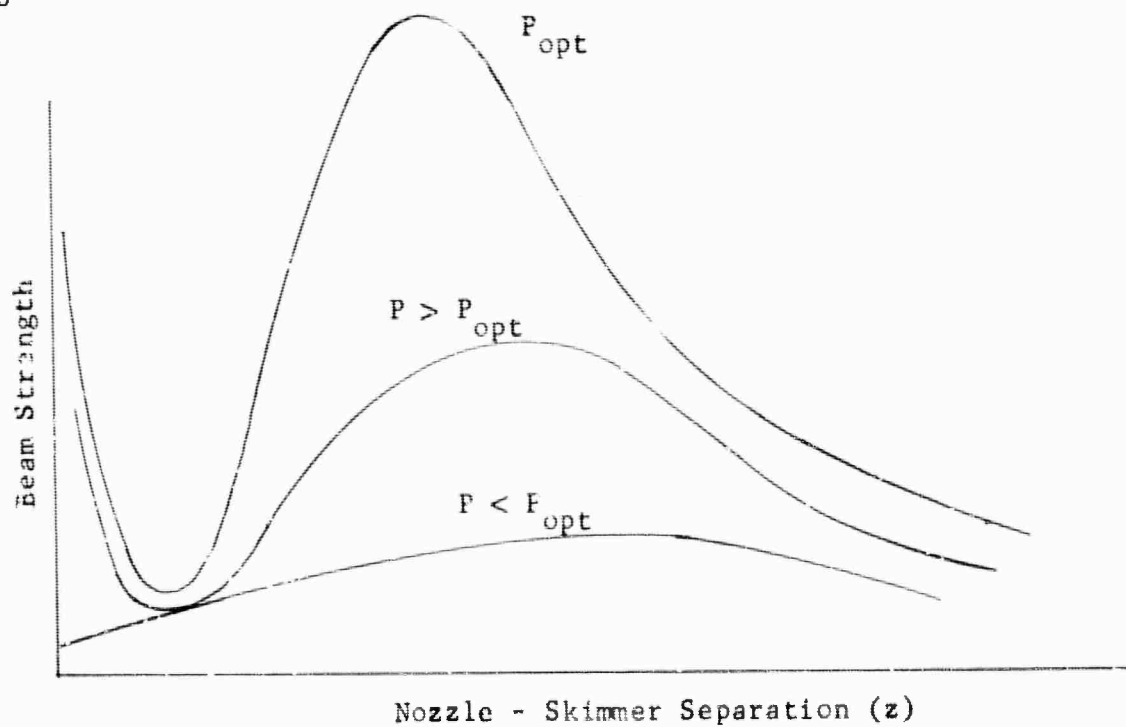
Fig. II-5.   a.   Diagram of Typical Aerodynamically Accelerated
                  Molecular Beam.

            b.   Typical Behavior of Beam Intensity at Detector
                 as a Function of Distance Between Nozzle and
                 Skimmer for Optimum and Non-Optimum Driving
                 Parameters.

The results are usually interpreted in terms of two limiting theories: one (Ref. 4) which describes the orifice flow and the other the molecular beam flow (Ref. 5) once it has entered the skimmer. It has been pointed out (Ref. 2) that the predictions of this compound theory are generally too high, often by large factors.

The conclusions which we have reached are that these two theories are incompatible except under certain matched conditions and that when these conditions are met the predictions are quite respectable. The behavior outside these match points can at least be qualitatively (semi-quantitatively in some cases) explained in terms of the flow regimes incolved and the conditions for optimum operation predicted quite reliable. Our conclusions are that the best beam operation is obtained, and beam strength is predictable, if the following conditions are met: (1) For a given driving pressure the separation of orifice and skimmer are such that the jet from the orifice just enters the slip flow regime. (2) The background pressure density in the first chamber is low compared with this density. (3) The best combination of driving pressure and orifice separation is obtained when this density is the highest compatible with molecular flow through the skimmer. (4) The total mass flow must be sufficiently high so that the jet is appreciably larger than the skimmer orifice diameter. This is consistent with the physical picture that optimum operation is obtained with a beam source of maximum density consistent with molecular flow at the skimmer and the absence of shock losses at the skimmer mouth. (Possible regimes of operation are shown in Table II). This is also the only regime where both theories would be expected to give reasonable predictions, since the orifice theory is essentially continuum while the beam theory is molecular.

These conclusions are being formalized in the form of a paper which is under preparation.

BLANK PAGE

Table II. FLOW REGIME IN TYPICAL

Jet	Skimmer Throat	
(1) Cont.	Cont. (Swallowed shock)	
(2) Cont.	Cont. (Swallowed shock)	
(3) Cont.	Cont. (Swallowed shock)	
(4) Cont.	Molecular (Bow shock)	M (S
(5) Trans.	Molecular	M
(6) Molecular	Molecular	M

ICAL AERODYNAMICALLY ACCELERATED MOLECULAR BEAMS.

Beam-1	Collimator Throat	Beam-2
Cont.	Cont. (Swallowed shock)	Cont. (Expansion to molecular spray)
Cont.	Molecular (Bow chock)	Molecular (Stagnation beam)
Trans.	Molecular	Molecular
Molecular (Stag. Beam)	Molecular	Molecular
Molecular	Molecular	Molecular
Molecular	Molecular	Molecular "Over beam"

References

1. E. W. Becker and W. Henkes, Z. Physik. 146, 320 (1956).

2. J. Deckers and J. B. Fenn, Rev. Sci. Inst. 34, 96 (1963).

3. Task R Quarterly Progress Report No. 20, APL/JHU SR 4-4, (Jan.-March 1964).

4. P. L. Owen and C. K. Thornhill, "The Flow In and Axially Symmetric Supersonic Jet From a Nearly Sonic Orifice Into a Vacuum," Armament Research Establishment Report No. 30/48, Ministry of Supply, Great Britain (Sept. 1948).

5. H. M. Parker, A. R. Kulthau, R. N. Zapata, and J. E. Scott, Jr., Proceedings of the First International Rarefied Gas Dynamics Symposium, Pergamon Press, New York (1960) p. 69.

III. ROCKET NOZZLE FLUID DYNAMICS

(H. J. Unger)

Objective

The fluid dynamic and chemical processes which occur in rocket nozzle flow are of fundamental interest for design purposes and the reason for this investigation is to collect experimental data for more exact description. Solid propellants have been used as a source to produce typical combustion conditions for a particular nozzle and various measurements are taken in the supersonic portion downstream from the throat. The gas generated is complex in species, making the fluid properties difficult to predict from simple thermodynamics. The gas is in chemical equilibrium dependent on temperature so the composition varies with position along the nozzle axis. Location of the position where the system goes out of equilibrium includes measurement of the fluid dynamic properties of the flow and the concentration of species in the gas mixture.

Fluid dynamic studies require flow surveys made by using techniques common to supersonic and hypersonic wind tunnels. From these measurements detailed boundary layer data in the nozzle is obtained. In proximity and at the throat optical pyrometry has been employed to obtain surface temperatures and temperature gradients below the surface. These data give heat transfer rates which allow calculation of the conventional coefficients of heat transfer and skin friction. Measurement of species concentrations in the flow are made with an infrared rapidly scanning spectrometer. Observation is accomplished by cutting slit-windows in the nozzle walls at suitable stations; thus it is possible to view the flow as a function of distance along the axis and record both the absorption and emission spectra in a selected wavelength region.

Because of mutual effects of the gas species a suitable set of calibration data is required before one may find the concentration of one ormore of the constituents. The concentration data are ther correlated with kinetic theory calculations to determine the equilibrium properties of the gas flow.

Spectrography

The experimental work on the adaption of infrared spectroscopic techniques to high temperature rocket tunnel research has gone through three stages, feasibility, test and calibration. For the past year all of the effort has been expended on the calibration phase because sufficient experimental data had been accumulated on the rocket nozzle survey. Because the Beer-Lambert law does not hold over a wide range of pressure and temperature for mixtures of gases, or for a simple species, it was necessary to calibrate with simulator systems. A heated free jet was used for CO_2-N_2 and CO-N_2 mixtures at atmospheric pressure, while a static cell in an electric furnace was used at pressures from 2 lbs/in^2 to 175 lbs/in^2 and temperatures up to 1300°C. Both emission and absorption measurements were made on a series of CO_2-N_2 mixtures bracketing the range of concentrations expected to exist in the rocket tunnel.

CO_2 was chosen as the first gas of the mixture to calibrate because the 4.26μ band is very sensitive to concentration changes. Also, CO_2 is easier to handle than CO or even H_2O. Another advantage is that more work has been done on CO_2 than on any other gas. The heart of this calibration equipment was the high temperature cell. A relatively complete description of the cell and furnace was given in Ref. 1). In general, every test involves rebuilding the cell as well as the furnace because of the brute force method sealing the sapphire windows to the molybdenum and the overheating of the electrical units. These units were designed for 1200°C maximum but have been successfully operated at 1300°C for a period of hours. The sapphire windows show slippage at the optical

surface and usually cleave when reheated. For this reason they are seldom reused. About one-third of the cell windows go through a test cycle intact and have been resurfaced and used a second time when new windows were not available.

A complete series of static cell tests have now been completed using 0.5", 1.0" and 2.0" path lengths, pressures from 2 psia to 175 psia, temperatures from ambient to 1300°C, and CO_2 concentrations from 2.5% to 20% by volume. These data cover a range of ρl (density $\times$ path length) values that bracket most all of the high temperature tunnel data observed and previously reported.

In all of the static cell tests it has been observed that the cell windows became fogged by condensation of products from the insulation and heaters. Sometimes the deposits were on the inside of the external windows and sometimes on both. Various conditions were imposed on the inner volume of the furnace from vacuum to 50 psia of nitrogen. Since the deposits always appeared on the outside of the cell and seemed to come from the hottest area of the heater, it was decided to connect a continuous tube of molybdenum from the cell windows to the furnace windows and thus isolate the source of contamination. This strategy worked very well but then the cell windows became opaque because a mirror-like hard metallic coating appeared on the inside of the cell. The heaters burned out at a cell temperature of about 1400°C and investigation revealed that arcing from the heater to the 1/8" molybdenum side-tubes of the cell had occurred. It is apparent that evaporation was the cause of the metallic deposit on the windows. Another attempt may be made to attain the high temperature goal.

On June 4th the 193rd rocket tunnel test was conducted for the purpose of checking the information obtained from TN 173. The absorption of CO_2 at 4.24μ at the 1.25" station appeared to be out of line with the data from other stations and it appeared advisable to repeat the test. After an eighteen months interim the absorption values checked with 0.1%

TN 173   abs. CO_2 at 4.24μ = 96.2 ± 0.3%

TN 193   "   " "   "   = 96.1 ± 0.4%

This repeatability reaffirms our faith in the accuracy of this measuring technique.

From the spectrometer calibration data obtained from the free jet (Ref. 2) and the static absorption cell for CO_2 in N_2 the amount of CO_2 in the rocket tunnel at four stations has been determined as shown in Fig. III-1. The data for each station were obtained from twelve spectrograms from each test. The brackets show the maximum variation at each station or temperature, and there appeared to be no trend during a particular test; i.e. the gas composition at a particular station showed no tendency to rise or fall. Most of the propellant charges used in this series of tests were from the same batch and casting. Great care was taken to assure analytic uniformity; even the ignitors used were proof tested by A.B.L. before acceptance by this laboratory.

Fig. III-1 shows that the CO_2 content of the exhaust gas from the ARP lies between the equilibrium and the frozen kinetic curves but very close to the latter. It is not known whether the tendency for the experimental curve to bend away and then back towards the frozen kinetic curve is real or not.

References

1. Task R Quarterly Progress Report No. 20, APL/JHU SR 4-4.
2. Task R Quarterly Progress Report No. 18, APL/JHU SR 4-2.
3. A. A. Westenberg and S. Favin, Ninth International Symposium on Combustion, Academic Press, New York (1963) p. 785.
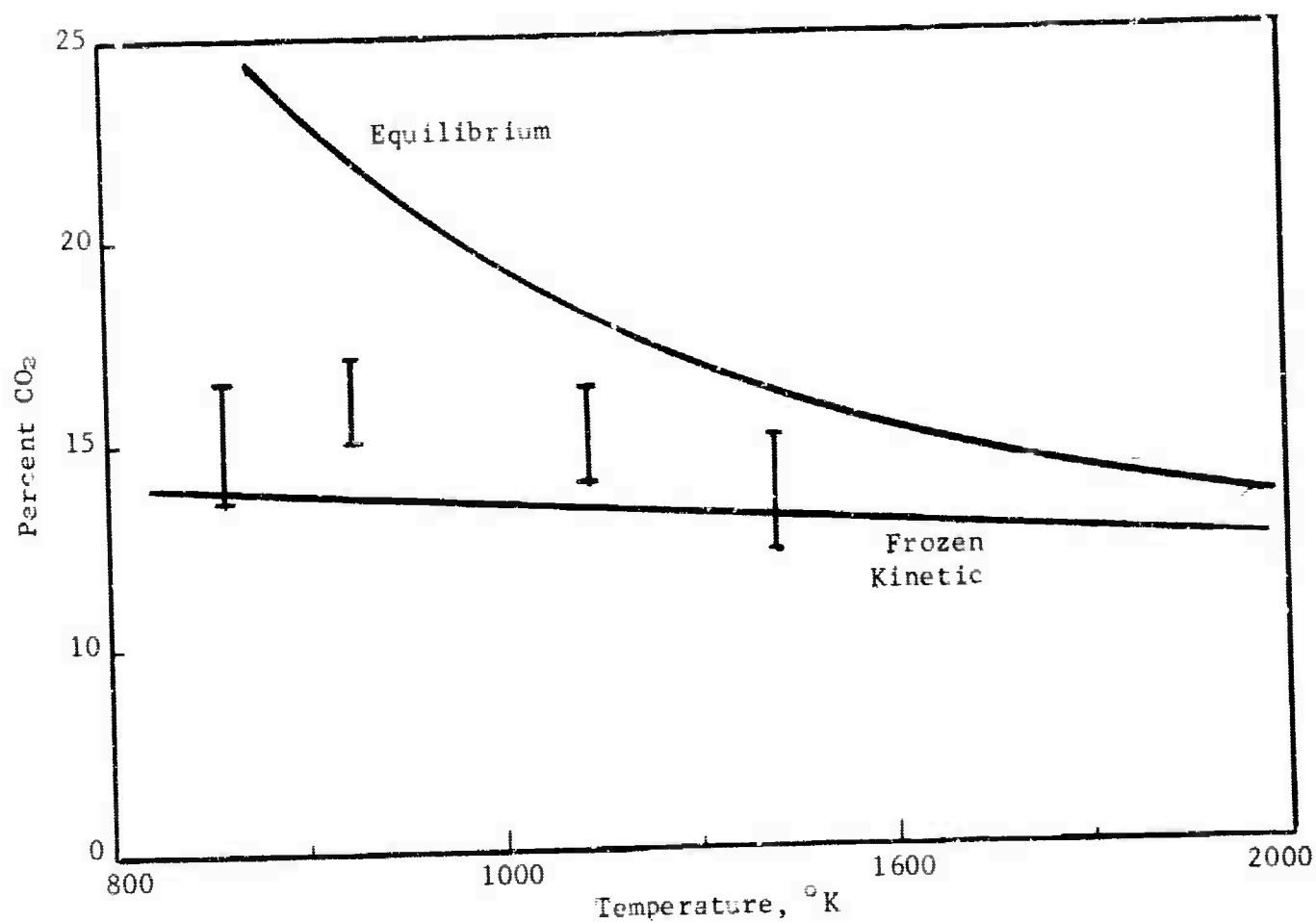
Fig. III-1. CO_2 Concentration as a Function of Temperature in the Rocket Nozzle. The equilibrium calculation assumes chemical equilibrium at all points in the nozzle, while the kinetic calculation utilizes the reaction rates assumed to hold for the individual species involved as shown in Reference 3.

Initial distribution of this document has been made
in accordance with a list on file in the Technical Reports
Group of The Johns Hopkins University, Applied Physics
Laboratory.